



HAL
open science

Nonlinear Locally Adaptive Wavelet Filter Banks

Gerlind Plonka, Stefanie Tenorth

► **To cite this version:**

Gerlind Plonka, Stefanie Tenorth. Nonlinear Locally Adaptive Wavelet Filter Banks. SAMPTA'09, May 2009, Marseille, France. pp.Poster session. hal-00453553

HAL Id: hal-00453553

<https://hal.science/hal-00453553>

Submitted on 5 Feb 2010

HAL is a multi-disciplinary open access archive for the deposit and dissemination of scientific research documents, whether they are published or not. The documents may come from teaching and research institutions in France or abroad, or from public or private research centers.

L'archive ouverte pluridisciplinaire **HAL**, est destinée au dépôt et à la diffusion de documents scientifiques de niveau recherche, publiés ou non, émanant des établissements d'enseignement et de recherche français ou étrangers, des laboratoires publics ou privés.

Nonlinear Locally Adaptive Wavelet Filter Banks

Gerlind Plonka ⁽¹⁾ and Stefanie Tenorth ⁽¹⁾

(1) Department of Mathematics, University of Duisburg-Essen, 47048 Duisburg, Germany.
gerlind.plonka@uni-due.de, stefanie.tenorth@uni-due.de

Abstract:

In this paper we introduce a new construction of nonlinear locally adaptive wavelet filter banks by connecting the lifting scheme with the idea of image smoothing by nonlinear diffusion methods.

1. Introduction

A crucial problem in data analysis is to construct efficient low-level representations, thereby providing a precise characterization of features which compose it, such as edges and texture components. Fortunately, in many relevant applications, the components of given multidimensional data are not independent, and the strong correlation between neighboring data points can be suitably exploited. In the two-dimensional case, tensor-product wavelets are not optimal for representing geometric structures because their support is not adapted to directional geometric properties.

Instead of choosing a priori a basis or a frame to approximate the image, one can try to adopt the approximation scheme to the image geometry. Within the last years, different approaches have been developed in this direction, see e.g. [1, 4, 5, 7, 10, 12, 13]. In particular, the construction of non-linear filter banks by the lifting scheme has been proposed already in [4, 8]. Since that time, there have been different attempts to construct adaptive and directional lifting based, invertible transforms for sparse image representation, see [2, 5, 6, 9, 12]. The lifting scheme for representation of wavelet filter banks has originally been suggested and analyzed by Sweldens [16]. It provides a flexible tool for the construction of new nonlinear wavelet filter banks. The main feature of lifting is that it provides an entirely spatial-domain interpretation of the transform. Besides wavelet shrinkage, other approaches like regularization techniques and PDE-based methods (as nonlinear diffusion) have been shown to be powerful tools in signal and image restoration in image processing, e.g., for denoising purposes. In particular, the choice of nonlinear diffusion filters leads to impressive results by removing insignificant, small-scale variations while preserving important features such as discontinuities [3, 11, 17, 18]. In [15], certain connections between explicit discrete one-dimensional schemes for non-linear diffusion and shift-invariant Haar wavelet shrinkage have been established.

In this paper we wish to construct a new invertible nonlinear wavelet filter bank by connecting the two concepts of the lifting scheme and the discrete nonlinear diffusion. The main goal is to adapt the local geometry of images suitably, in order to obtain highly efficient sparse image representations.

2. Lifting and Nonlinear Diffusion

2.1 The Lifting Scheme

The typical lifting scheme consists of three steps: Split, Predict and Update.

1. Split. Usually, in this step, the given data is split into even and odd components. Let $N \in \mathbb{N}$ be of the form $N = 2^l r$ with $l, r \in \mathbb{N}$. For a given digital image of the form $a = (a(i, j))_{i, j=0}^{N-1} \in \mathbb{R}^{N \times N}$, we split the data into the following two sets of equal size,

$$\begin{aligned} a^e &:= (a_{i, j})_{i, j=0, i+j \text{ even}}^{N-1}, \\ a^o &:= (a_{i, j})_{i, j=0, i+j \text{ odd}}^{N-1} \end{aligned}$$

and we denote the components of a^e and a^o by $a_{i, j}^e$ and $a_{i, j}^o$, respectively. The data sets a^e and a^o split the image a like a checkerboard.

2. Predict. The goal of the prediction step is to find a good approximation \tilde{a}^o of the data a^o of the form

$$\tilde{a}^o = P_1(a^o) + P_2(a^e).$$

Here P_1 and P_2 can be nonlinear operators. Afterwards, we consider the residual

$$d^o := a^o - \tilde{a}^o = a^o - (P_1(a^o) + P_2(a^e)).$$

We have to assume that the mapping $(a^e, a^o) \mapsto (a^e, d^o)$ is invertible, i.e., the operator $I - P_1$ needs to be invertible for arbitrary data a^o . The operators P_1 and P_2 need to be chosen such that the residual d^o is very small.

3. Update. In the third step, we aim to find a smoothed approximation of the data a^e that can be regarded as a low-pass filtered and subsampled version of the original image a . The general update has the form

$$\tilde{a}^e := U_1(d^o) + U_2(a^e)$$

with (possibly nonlinear) operators U_1 and U_2 , where we again want to assume the invertibility of the mapping

$(a^e, d^o) \mapsto (\tilde{a}^e, d^o)$, i.e., U_2 is assumed to be invertible such that

$$a^e = U_2^{-1}(\tilde{a}^e - U_1(d^o)).$$

The complete scheme is illustrated in Figure 1.

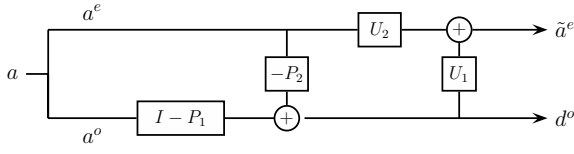


Figure 1: Illustration of the nonlinear filter bank using the lifting scheme.

2.2 Nonlinear Diffusion

The nonlinear diffusion has been shown to be a very successful model for image denoising. For $\Omega = (0, N_1) \times (0, N_1)$ we consider the diffusion equation

$$\frac{\partial u}{\partial t} = \text{div} \left(g(|\nabla u|) \nabla u \right) \quad \text{on } \Omega \times (0, \infty) \quad (1)$$

with a given noisy image a as initial state

$$u(x, 0) = a(x), \quad x \in \overline{\Omega}$$

and with Neumann boundary conditions $\frac{\partial u}{\partial n} = 0$ on $\partial\Omega$. Here, $\nabla u = (u_{x_1}, u_{x_2})^T = (\partial u / \partial x_1, \partial u / \partial x_2)^T$ denotes the gradient of u , and $|\nabla u| := \sqrt{u_{x_1}^2 + u_{x_2}^2}$. The time t in (1) is a scale parameter. Increasing t corresponds to stronger filtering. The diffusivity function $g(|\nabla u|)$ is a non-negative function that determines the amount of diffusion. It is decreasing in $|\nabla u|$ in order to ensure that strong edges are hardly blurred by the diffusion filter while small variations (noise) are smoothed much stronger. Frequently used bounded diffusivities are the Perona-Malik diffusivity

$$g(x) := \frac{1}{1 + x^2 / \lambda^2},$$

or the Weickert diffusivity

$$g(x) := \begin{cases} 1 & x = 0, \\ 1 - \exp\left(\frac{-3.315}{(x/\lambda)^4}\right) & x > 0, \end{cases}$$

see [14, 17]. One may also take a ‘‘robust’’ diffusivity of the form

$$g(x) := \begin{cases} 1 & 0 \leq x < \theta, \\ 0 & |x| \geq \theta, \end{cases}$$

as it has been used in [14] with a suitably chosen threshold θ .

Replacing $g(|\nabla u|)$ by $g(|\nabla u_\sigma|)$, where u_σ denotes the slightly smoothed image by convolution with the Gaussian kernel, $u_\sigma := K_\sigma \star u$, existence and uniqueness of a solution of (1) have been shown in [3].

For application of the diffusion approach to digital images we follow [11] and replace (1) by the following slightly modified equation

$$\frac{\partial u}{\partial t} = \partial_{x_1} (g(|\partial_{x_1} u|) \partial_{x_1} u) + \partial_{x_2} (g(|\partial_{x_2} u|) \partial_{x_2} u).$$

We use a discretization of the form

$$\begin{aligned} \frac{u_{i,j}^{k+1} - u_{i,j}^k}{\tau} &= g(|u_{i+1,j}^k - u_{i,j}^k|)(u_{i+1,j}^k - u_{i,j}^k) \\ &\quad - g(|u_{i,j}^k - u_{i-1,j}^k|)(u_{i,j}^k - u_{i-1,j}^k) \\ &\quad + g(|u_{i,j+1}^k - u_{i,j}^k|)(u_{i,j+1}^k - u_{i,j}^k) \\ &\quad - g(|u_{i,j}^k - u_{i,j-1}^k|)(u_{i,j}^k - u_{i,j-1}^k), \end{aligned} \quad (2)$$

where $u_{i,j}^0 := a_{ij}$ for $i, j = 0, \dots, N-1$. Here, k denotes the iteration step and τ is the step size of time discretization. In our numerical examples we will use the step size $\tau = 1/4$.

3. The Nonlinear Diffusion Filter Bank

Now we want to apply the nonlinear diffusion filter for the construction of prediction and update operators in the lifting scheme, in order to obtain a new sparse representation of images. The nonlinear filter bank should satisfy the following demands.

1. For linear (bivariate) polynomials, the residual d^o found in the prediction step should vanish. This condition is equivalent with two vanishing moments of the high-pass filter in a wavelet filter bank.
2. Near discontinuities (edges) of u , the residual d^o should remain small.
3. The data \tilde{a}^e should be a suitable (downsampled) approximation of the image a with good low-pass filter properties in smooth areas of a and without blurring of edges.

3.1 Choice of the Prediction Operator

Using equation (2) with the notations $a_{i,j}^o := u_{i,j}^0$, $\tilde{a}_{i,j}^o := u_{i,j}^1$ for $i+j$ odd, and $a_{i,j}^e := u_{i,j}^0$ for $i+j$ even, we obtain

$$\begin{aligned} \tilde{a}_{i,j}^o &= a_{i,j}^o + \tau \left[g(|a_{i+1,j}^e - a_{i,j}^o|)(a_{i+1,j}^e - a_{i,j}^o) \right. \\ &\quad + g(|a_{i-1,j}^e - a_{i,j}^o|)(a_{i-1,j}^e - a_{i,j}^o) \\ &\quad + g(|a_{i,j+1}^e - a_{i,j}^o|)(a_{i,j+1}^e - a_{i,j}^o) \\ &\quad \left. + g(|a_{i,j-1}^e - a_{i,j}^o|)(a_{i,j-1}^e - a_{i,j}^o) \right]. \end{aligned}$$

A prediction could now be of the form

$$\begin{aligned} d_{i,j}^o &= a_{i,j}^o - \tilde{a}_{i,j}^o \\ &= -\tau \left[\sum_{\substack{\mu, \nu = -1 \\ |\mu| + |\nu| = 1}}^1 g(|a_{i+\mu, j+\nu}^e - a_{i,j}^o|)(a_{i+\mu, j+\nu}^e - a_{i,j}^o) \right]. \end{aligned}$$

Unfortunately, with this choice of prediction the desired invertibility of the mapping $(a^e, a^o) \mapsto (a^e, d^o)$ is not guaranteed since the nonlinear diffusion g depends on the data $a_{i,j}^o$. Therefore, we replace the values $a_{i,j}^o$ that are used for the computation of the function values of g by the median of its four direct neighbors,

$$a_{i,j}^o \approx \text{median} \{a_{i,j+1}^e, a_{i,j-1}^e, a_{i+1,j}^e, a_{i-1,j}^e\} := \text{med } a_{i,j}^o.$$

A normalization with

$$g_{ij} := \sum_{\substack{\mu, \nu = -1 \\ |\mu| + |\nu| = 1}}^1 g(|a_{i+\mu, j+\nu}^e - \text{med } a_{i,j}^o|)$$

now yields the prediction

$$\begin{aligned} d_{i,j}^o &:= \frac{-\tau}{g_{ij}} \sum_{\substack{\mu,\nu=-1 \\ |\mu|+|\nu|=1}}^1 g(|a_{i+\mu,j+\nu}^e - \text{med } a_{i,j}^o|) (a_{i+\mu,j+\nu}^e - a_{i,j}^o) \\ &= \tau a_{i,j}^o - \frac{\tau}{g_{ij}} \sum_{\substack{\mu,\nu=-1 \\ |\mu|+|\nu|=1}}^1 g(|a_{i+\mu,j+\nu}^e - \text{med } a_{i,j}^o|) a_{i+\mu,j+\nu}^e. \end{aligned}$$

Now, the invertibility of the prediction is ensured for $\tau > 0$ and we have

$$a_{i,j}^o = \frac{d_{i,j}^o}{\tau} + \frac{1}{g_{ij}} \sum_{\substack{\mu,\nu=-1 \\ |\mu|+|\nu|=1}}^1 g(|a_{i+\mu,j+\nu}^e - \text{med } a_{i,j}^o|) a_{i+\mu,j+\nu}^e.$$

Observe that the term g_{ij} is positive for all i, j if we take Perona-Malik diffusivity or Weickert diffusivity. At the boundary of the image, where not all four neighbors of a data point are given, we slightly change the operator and use only the three available neighbors in the sum (or even only two neighbors at a vertex). Because of the normalization with the (correspondingly defined constants g_{ij}) the properties of the prediction operator will not change.

3.2 Choice of the Update Operator

As update operator we simply apply a linear operator of the form

$$\tilde{a}_{i,j}^e = \sqrt{2} a_{i,j}^e + \frac{1}{4} (d_{i+1,j}^o + d_{i-1,j}^o + d_{i,j+1}^o + d_{i,j-1}^o).$$

Invertibility is obviously satisfied and we find

$$a_{i,j}^e = \frac{1}{\sqrt{2}} (\tilde{a}_{i,j}^e - \frac{1}{4} (d_{i+1,j}^o + d_{i-1,j}^o + d_{i,j+1}^o + d_{i,j-1}^o)).$$

At the boundary, where $a_{i,j}^e$ has only three neighbors, we slightly change the operator. For example, for $0 < i < N - 1$ and $j = 0$, we take

$$\tilde{a}_{i,0}^e := \sqrt{2} a_{i,0}^e + \frac{1}{3} (d_{i+1,0}^o + d_{i-1,0}^o + d_{i,1}^o),$$

etc.. Analogously, at vertices, only two neighbors are taken into account.

Observe that the low-pass filtered values $\tilde{a}_{i,j}^e$ are amplified by $\sqrt{2}$ here (as it is usual also for orthogonal wavelet filter banks).

3.3 Iterative Application of the Filter Bank

In order to obtain a suitable sparse representation of the digital image a , we now iteratively apply the nonlinear filter bank described above, and we use a hard threshold procedure to suppress small residual values $d_{i,j}^o$.

After the first application of the filter bank, the (small) residual data $d_{i,j}^o$, $i, j = 0, \dots, N - 1$, $i + j$ odd, are stored and we consider only the $N^2/2$ values $\tilde{a}_{i,j}^e$, $i, j = 0, \dots, N - 1$, $i + j$ even. For a second application of the filter bank to $\tilde{a}_{i,j}^e$, we rename these data by $a_{k,l}^{(1)} := \tilde{a}_{k-l,k+l}^e$, where $k = 0, \dots, N - 1$ and $l = -\min\{k, N - 1 - k\}, \dots, \min\{k, N - 1 - k\}$, and apply the filters now to this data set, etc..

As usual, the complete procedure involves the following three steps. First, we decompose the image by an iterative

application of the diffusion filter bank. Secondly, we apply the shrinkage function

$$S_\theta(x) := \begin{cases} x & |x| \geq \theta, \\ 0 & |x| < \theta, \end{cases}$$

to the residual coefficients. In our numerical experiments we will take a level-independent threshold θ . Finally, we reconstruct the image with the modified residual coefficients.

4. Properties of the Diffusion Filter Bank

We can show the following

Theorem 1.

Let g be a diffusivity function satisfying $0 < g(|x|) \leq 1$ for $x \in \mathbb{R}$. The diffusion filter bank determined in Section 3 reproduces linear polynomials.

Proof. We consider a linear polynomial of the form

$$a(x_1, x_2) = a_0 + b_0 x_1 + c_0 x_2, \quad a_0, b_0, c_0 \in \mathbb{R}.$$

Let the digital image now be given by

$$a_{i,j} = a(ih, jh) = a_0 + b_0 ih + c_0 jh.$$

Then we obtain for data that are not at the boundary

$$\begin{aligned} \text{med } a_{i,j}^o &= \text{median} \{a_0 + b_0(i-1)h + c_0 jh, a_0 + \\ &\quad b_0(i+1)h + c_0 jh, a_0 + b_0 ih + c_0(j-1)h, \\ &\quad a_0 + b_0 ih + c_0(j+1)h\} \\ &= a_0 + b_0 ih + c_0 jh + \\ &\quad \text{median} \{-b_0 h, b_0 h, -c_0 h, c_0 h\} \\ &= a_0 + b_0 ih + c_0 jh = a_{i,j}^o \end{aligned}$$

and

$$\begin{aligned} d_{i,j}^o &= \frac{-\tau}{g_{ij}} \sum_{\substack{\mu,\nu=-1 \\ |\mu|+|\nu|=1}}^1 g(|a_{i+\mu,j+\nu}^e - a_{i,j}^o|) (a_{i+\mu,j+\nu}^e - a_{i,j}^o) \\ &= \frac{-\tau}{g_{ij}} [g(b_0 h)(a_{i+1,j}^e + a_{i-1,j}^e - 2a_{i,j}^o) \\ &\quad + g(c_0 h)(a_{i,j+1}^e + a_{i,j-1}^e - 2a_{i,j}^o)] \\ &= 0. \end{aligned}$$

Hence the prediction operator leads to $d_{i,j}^o = 0$ and the update yields $\tilde{a}_{i,j}^e = \sqrt{2} a_{i,j}^e$ for all i, j with $i + j$ even. \square

Further, one can show in case studies, that the proposed filter bank behaves well at vertical, horizontal and diagonal edges, i.e., the obtained residual values using the nonlinear prediction operator remain to be small.

5. Numerical Results

We apply the above described nonlinear diffusion filter bank in order to achieve sparse image representations. In the experiment, we consider the monarch image. We use the Perona-Malik diffusivity with $\lambda = 28$ and with $\tau = 0.25$. We apply 8 levels of the nonlinear filter bank,

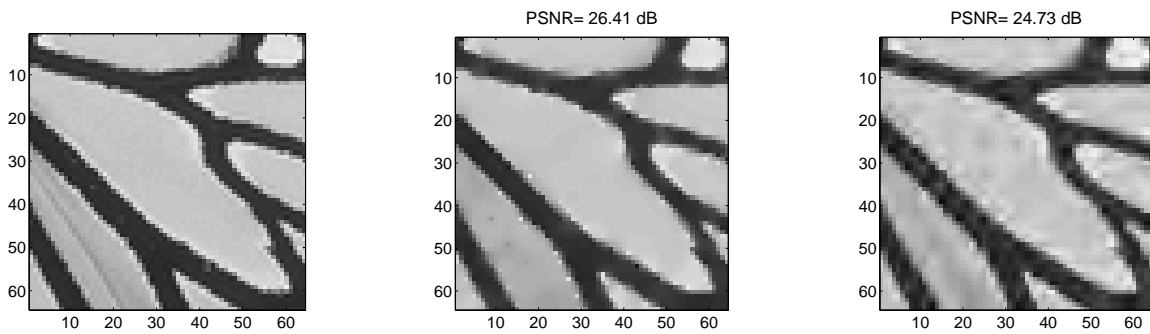


Figure 2: Original image Monarch (left), sparse image representation with 449 coefficients using the proposed nonlinear diffusion filter bank (middle) and the biorthogonal filter bank with 7-9 filter (right).

i.e., there will remain 16 low-pass coefficients. For thresholding we use the hard shrinkage function with $\theta = 13$. In Figure 2(left), we present the original image. Figure 2(middle) shows the obtained compressed image with 449 remaining coefficients using the new diffusion filter bank. For comparison, we apply 8 decomposition levels of the two-dimensional biorthogonal wavelet shrinkage with the 7–9 filter with the same number of 449 remaining nonzero coefficients, see Figure 2(right). As we can see, the nonlinear filter bank not only gives an optically better result but also achieves a better PSNR value (26.41 dB) while the biorthogonal filter bank achieves a PSNR of 24.73 dB. We remark that our method is especially designed for constructing efficient low-level representations and does not work well for image denoising.

6. Acknowledgement

The research in this paper is supported by the project PL 170/13-1 of the German Research Foundation (DFG). This is gratefully acknowledged.

References:

- [1] F. Arandiga, A. Cohen, R. Donat, N. Dyn. Interpolation and approximation of piecewise smooth functions. *SIAM J. Numer. Anal.* 43:41–57, 2005.
- [2] N.V. Boulgouris, D. Tzovaras, and M.G. Strintzis. Lossless image compression based on optimal prediction, adaptive lifting, and conditional arithmetic coding. *IEEE Trans. Image Process.* 10:1–14, 2001.
- [3] F. Catté, P.-L. Lions, J.-M. Morel, and T. Coll. Image selective smoothing and edge detection by nonlinear diffusion. *SIAM J. Numer. Anal.* 29:182–193, 1992.
- [4] R.L. Claypoole, G.M. Davis, W. Sweldens, and R.G. Baraniuk. Nonlinear wavelet transforms for image coding via lifting. *IEEE Trans. Image Process.* 12:1449–1459, 2003.
- [5] A. Cohen and B. Matei. Compact representation of images by edge adapted multiscale transforms. In *Proc. IEEE Int. Conf. on Image Process. (ICIP)*, Thessaloniki, pages 8–11, 2001.
- [6] W. Ding, F. Wu, X. Wu, S. Li, and H. Li. Adaptive directional lifting-based wavelet transform for image coding. *IEEE Trans. Image Process.* 16:416–427, 2007.
- [7] D.L. Donoho. Wedgelets: Nearly minimax estimation of edges. *Ann. Stat.* 27:859–897, 1999.
- [8] F.J. Hampson and J.-C. Pesquet. A nonlinear subband decomposition with perfect reconstruction. *Proc. IEEE Int. Conf. Acoust., Speech, and Signal Proc.*, pages 1523–1526, 1996.
- [9] H.J.A.M. Heijmans, B. Pesquet-Popescu, G. Piella. Building nonredundant adaptive wavelets by update lifting. *Appl. Comput. Harmon. Anal.* 18:252–281, 2005.
- [10] S. Mallat. Geometrical grouplets. *Appl. Comput. Harmon. Anal.* 26:161–180, 2009.
- [11] P. Perona and J. Malik. Scale space and edge detection using anisotropic diffusion. *Proc. IEEE Computer Society Workshop on Computer Vision*, IEEE Computer Society Press, pages 16–22, 1987.
- [12] G. Piella, B. Pesquet-Popescu, H.J.A.M. Heijmans, and G. Pau. Combining seminorms in adaptive lifting schemes and applications in image analysis and compression. *J. Math. Imaging Vis.* 25:203–226, 2006.
- [13] G. Plonka. The easy path wavelet transform: A new adaptive wavelet transform for sparse representation of two-dimensional data. *Multiscale Model. Simul.* 7:1474–1496, 2009.
- [14] G. Plonka and J. Ma. Convergence of an iterative nonlinear scheme for denoising of piecewise constant images. *Int. J. Wavelets Multiresolut. and Inf. Process.* 5:975–995, 2007.
- [15] G. Steidl, J. Weickert, T. Brox, P. Mrázek, M. Welk. On the equivalence of soft wavelet shrinkage, total variation diffusion, total variation regularization, and sides. *SIAM J. Numer. Anal.* 42/2:686–713, 2004.
- [16] W. Sweldens. The lifting scheme: A construction of second generation wavelets. *SIAM J. Math. Anal.* 29:511–546, 1997.
- [17] J. Weickert. *Anisotropic Diffusion in Image Processing*. Teubner, Stuttgart, 1998.
- [18] M. Welk, G. Steidl, and J. Weickert. A four-pixel scheme for singular differential equations. In R. Kimmel, N. Sochen, J. Weickert, editors, *Scale-Space and PDE Methods in Computer Vision*. Lecture Notes in Computer Science, Springer, Berlin, pages 610–621 (2005).